Tunneling evidence for spatial location of the charge-density-wave induced band splitting in 1*T*-$TaSe_2$

D. Stoltz,[1,*] M. Bielmann,[2] M. Bovet,[3] L. Schlapbach,[2] and H. Berger[4]
[1]*Materialfysik, MAP, KTH-Electrum, SE-16440 Kista, Sweden*
[2]*Swiss Federal Lab for Materials Science and Technology (EMPA), CH-8600 Dübendorf, Switzerland*
[3]*Institut de Physique, Université de Neuchâtel, CH-2000 Neuchâtel, Switzerland*
[4]*Institut de Physique Appliquée, EPF, 1015 Lausanne, Switzerland*
(Received 1 May 2007; revised manuscript received 31 May 2007; published 21 August 2007)

We present the atomically resolved room temperature scanning-tunneling microscopy study of bias dependent images of charge density waves (CDWs) in 1*T*-$TaSe_2$. With the help of angle-resolved photoemission of the CDW-split Ta d_{z^2} band in 1*T*-$TaSe_2$, we determine the electronic location of Ta d_{z^2} subbands on inequivalent atoms of the reconstructed Ta plane. We thus demonstrate the atomic origin of the CDW-formation related effects observed in the band structure of this material.

DOI: 10.1103/PhysRevB.76.073410 PACS number(s): 73.20.Mf, 68.37.Ef, 71.20.−b, 79.60.−i

The charge-density-wave (CDW) formation has been one of the most popular topics of the last decades due to interest in the mechanism behind the interplay of the complex structural and electronic changes. One of the convenient hosts of the CDWs are the layered transition metal dichalcogenides (TMDs) of the 1*T* type. The quasi-two-dimensionality of these materials allows straightforward interpretations of the band mapping in terms of the mapping of the initial bands of the crystal and it promises conditions for the Fermi surface nesting—one of the most popular mechanisms proposed to be responsible for the CDW formation. Furthermore, recent investigations reveal similar mechanisms behind the electronic instability driven pseudogap in high-temperature superconductors[1,2] and the pseudogapped Fermi surface in 1*T*-TMDs: $TaSe_2$ and TaS_2.[3,4]

The advantage of studying 1*T*-$TaSe_2$ originates from the fact that it is in commensurate CDW phase already at room temperature (RT). Scanning-tunneling microcopy (STM) on this compound has revealed so far the CDW wavelength $\lambda_{CDW}=12.6$ Å (Ref. 5) and the image of the CDW reconstruction,[6–10] stating that the atomic modulation gives minor contribution to the overall *z* deflection, which is dominated by the CDW. Kim *et al.*[6] were the first to apply scanning-tunneling spectroscopy (STS) to investigate fingerprints of the CDW-reconstructed band structure.

In this Brief Report, we present atomically resolved RT STM measurements on 1*T*-$TaSe_2$ in its CDW phase. By tuning the bias voltage of the STM image, we tunnel into different CDW-split subbands of the Ta d_{z^2} band. These subbands are identified by band mapping. We demonstrate that they are spatially located on three groups of inequivalent atoms by visualizing those atoms when tunneling at a bias voltage same as the subband binding energy.

STM experiments on 1*T*-$TaSe_2$ have been performed in a UHV system equipped with a UHV atomic force microscopy/STM scanning probe microscope from Omicron NanoTechnology operating at RT described elsewhere.[11] The images were taken in a constant height mode. Bias voltages are given with respect to the sample, i.e., positive bias means tunneling from occupied states. Band-mapping experiments have been performed using Vacuum Generators ESCALAB Mk II spectrometer at room temperature with monochromatized He I ($h\nu=21.2$ eV) photons[12] by means of computer controlled sequential sample rotation.[13] The energy and angular resolution were 20 meV and 0.5°, respectively. The accurate position of the Fermi level (E_F) has been determined on a polycrystalline copper sample. Surface reconstruction was checked by low energy electron diffraction. X-ray photoelectron diffraction was used to determine the sample orientation *in situ* with an accuracy of better than 0.5°. Samples of 1*T*-$TaSe_2$ have been prepared from the elements by reversible chemical reaction with iodine as a transport agent, between 950° (hot zone) and 900° (cold zone).[14] They were cleaved *in situ* at pressures in the lower 10^{-10} mbar region.

Figure 1 shows experimental results obtained, implementing angle-photoemission spectroscopy along the $\bar{\Gamma}\bar{M}$ (a) and $\bar{\Gamma}\bar{K}$ (b) directions and up to a binding energy of 2 eV. Spectra cover the range between (a) 0° and 50° or (b) −5° and 20°

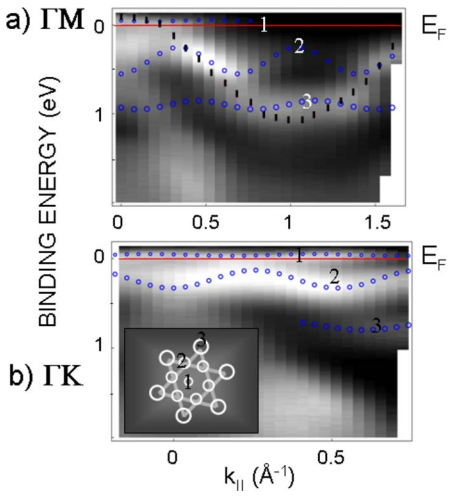

FIG. 1. (Color online) Band mapping along (a) $\bar{\Gamma}\bar{M}$ and (b) $\bar{\Gamma}\bar{K}$ of the cleaved 1*T*-$TaSe_2$ with a photon energy of 21.2 eV at RT. Dark circles represent the band splitting and folding with the new periodicity. Black markers highlight the schematic position of the unreconstructed band. High intensity in white.

in a given polar direction (converted to $k_{\|}$ in the image). The images depict dispersion of the Ta d_z^2 band, which exhibits a large electronlike pocket around the $\bar{M}$ point. At the higher binding energies, the Se $4p$ band appears energetically close to the Ta d_z^2 band primarily in the vicinity of $\bar{\Gamma}$ point.

Figure 1 shows that the Ta d_z^2 band [expected to disperse along ticks in Fig. 1(a)] is instead split into three subbands (circles). According to the Star-of-David model[15] of the $(\sqrt{13}\times\sqrt{13})R13.54°$ reconstruction in the Ta plane [Fig. 1(b), inset], the three subband manifolds are expected in the CDW phase. The formation of the stars breaks the hexagonal symmetry of the undistorted lattice and introduces three types of inequivalent atomic positions: the atom in the center (1), the six atoms constituting the first hexagon around it (2), and the six atoms constituting the outmost hexagon of the starlike cluster (3). These groups are assumed to correspond to different subband manifolds of the CDW-split Ta d_z^2 band [marked also as 1, 2, and 3 in Figs. 1(a) and 1(b)]. As the bands within the manifolds are not resolved, we will continue addressing the subband manifolds just as subbands.

The photoemission intensities follow the unreconstructed band structure[16] and thus highlight the three new subbands along the 1×1 dispersion:[4] high intensity of bands 1, 2, and 3 in Fig. 1(a) is mainly along the ticks marking the unreconstructed band. The new subbands are furthermore clearly backfolding: circles in Figs. 1(a) and 1(b) are following periodic functions with the periodicity of the new, reconstructed BZ and they describe the measured dispersion of the subbands astonishingly well. Both the band splitting and the backfolding of the subbands are CDW-related effects. A splitting of the Ta d band into oscillating subbands was confirmed by the *ab initio* band-structure calculations for the similar material—$1T$-TaS_2 (Ref. 4) with the CDW-induced atomic positions.

The periodic lattice distortion introduced by the CDW lock-in can be visualized by an STM. Figure 2 shows (a) 7×7 nm^2, (b) 8×6 nm^2, and (c) 7×6.6 nm^2 of the *in situ* cleaved $1T$-$TaSe_2$ surface measured with different bias voltages and a tunneling current of 1.2 nA.

Figure 2(a) at a bias voltage of 0.4 eV (tunneling from the occupied states) shows arrays of white flowerlike patterns. Their periodicity is ~12 Å, which corresponds to the diameter of one star drawn schematically in Fig. 1(b) (inset) and reproduced on the left side of Fig. 2. The periodic repetition of this pattern confirms the presence of the charge density waves. If we look at Fig. 1, the 0.4 eV binding energy corresponds mainly to the second subband. It is thus clear that by tunneling from the occupied states of one of the subbands, we achieve highest intensity on those atoms that electronically contribute to the chosen band. The resolution of Fig. 2(a) allows us to assign this subband to the first six atoms surrounding the central atom of the reconstruction (see arrows). It is clear from the image that the central atom as well as the outer six atoms are much less intense than the inner hexagon.

Figure 2(b) at a bias voltage of 0.2 V (tunneling from the occupied states) shows similar CDW pattern as in Fig. 2(a). In this image, the central atoms of the Star of David start to become the most intense, while the hexagon formed by the

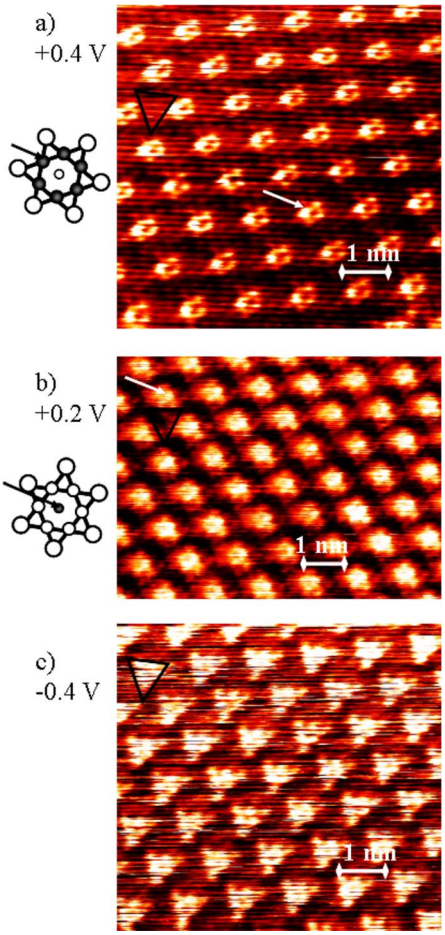

FIG. 2. (Color online) STM images of the cleaved $1T$-$TaSe_2$ surface taken at RT with 1.2 nA and (a) 0.4 V, (b) 0.2 V, and (c) −0.4 V. Images are (a) 7 nm, (b) 8 nm, and (c) 7 nm wide. High intensity in white.

first six atoms around the central one is still visible but much less intense than in Fig. 2(a). This can be explained by the correlation between the tunneling current and the electronic structure. The topmost subband is lying closest to 0.2 eV, which explains the intensity enhancement at the central atom (see arrows). However, even subband 2 contributes to the total intensity at this binding energy, which is why we see atoms of the first hexagon around the central atom, although less intense. Consequently, the outmost atomic hexagon in the Star of David is electronically responsible for the Ta d_z^2 subband with the largest binding energy.

Finally, in Fig. 2(c), a bias voltage of −0.4 V has been implemented to obtain the image. The image is dominated by triangularly shaped groups of atoms which still have the periodicity of the CDW-induced superstructure. There are several possible explanations for this. The lowest lying unoccupied bands are of $d_{x^2-y^2}$, d_{xy} character and should also undergo splitting due to the CDW [see calculations for TaS_2 (Ref. 4)]. If tunneling occurs into these bands, the spatial distribution of high intensity in the STM image should reveal their symmetry. Another possibility is that tunneling outside the Ta d_{z^2} band leaves most of the Star-of-David atoms in low intensity [dark areas in Fig. 2(c)], enhancing most out-

most atoms [compare triangles marked in Figs. 2(a)–2(c)]. This would be similar to the contrast reversal reported earlier in purple potassium molybdenum bronze.[17] In one previous study,[9] images with similar triangular atomic groups have been reported and explained by the changes in the electronic structure of the tip. In our study, these images have appeared only at a bias of −0.4 V.

Sacks *et al.*[18] have made an attempt to resolve the STM images of the CDW materials (such as $2H$-$NbSe_2$) by considering CDW effects on the band structure and thus on the tunneling. They state that several bands define the Fermi surface and that it will thus be tunneled from them all. Band degeneracy is taken to originate from band folding, while band splitting is disregarded. In our study we start from the band-mapping data which show energetically localized subbands of the Ta d_{z^2} band and which are interpreted in agreement with the band-structure calculations. Both band splitting and backfolding have influence on the formation of such subbands. Tunneling occurs thus primarily from a subband, in which the binding energy is the same as the bias.

In $1T$-$TaSe_2$ at room temperature, the slope of the temperature-dependent resistivity is metallic. Although $1T$-$TaSe_2$ does not show any metal-insulator transitions (MIT) at low temperatures, the surface MIT in $1T$-$TaSe_2$ has been recently reported at 200–250 K.[19,20] The CDW-induced band-structure changes lead to reduced bandwidth (W) and reduced W/U (U measures electron-electron interaction), which trigger a Mott-type transition.[19] Our measurements were performed at room temperature, in the electron-phonon interaction determined CDW ground state, which is also according to our STS measurements (not shown) metallic.

On the search for the driving mechanism of the CDW, the idea of the Peierls transition in a quasi-one-dimensional system has many times been considered even for a quasi-two-dimensional system such as $1T$-$TaSe_2$. However, this system is quasi-two-dimensional with threefold symmetry and the Peierls transition is not very likely. If we consider energetics of the CDW transition, the CDW-induced band splitting leads to new subbands which are energetically lower than the original Ta $5d$ band of the unreconstructed lattice.[4] The energy gained in this way can be used for elastic lattice distortion.

Our STM results support this idea. The conduction charge would be equally distributed over all Ta atoms in the unreconstructed lattice. Upon CDW transition, small changes in the atomic positions of all Ta atoms lead to periodic lattice distortion. In the CDW phase, we see that the conduction charge is mainly located on the central atom of the Star-of-David cluster, meaning that only 1 out of 13 atoms is contributing to the topmost band, which straddles the Fermi level. This can explain the resistivity jump related to the CDW transition in a rather obvious way. More than that, the stability of the CDW phase and the compensation of the lattice distortion energy clearly originate from the energetically lowered bands, which are spatially located on the remaining 12 atoms of the Star-of-David cluster and which are completely filled.

To conclude, band mapping of $1T$-$TaSe_2$ along $\bar{\Gamma}\bar{M}$ and $\bar{\Gamma}\bar{K}$ reveals CDW-induced splitting and folding of the Ta d_z^2 band into three subbands. Tunneling from separate subbands allows direct visualization of the atoms contributing to CDW-split electronic states. We thus assign the atoms of the Star-of-David cluster to the Ta d_z^2 subbands as follows: the topmost subband is electronically located on the central atom, the outer hexagon is the principal charge carrier of the second subband, and the outmost hexagon is thus related to the third subband. The relevance of this result is discussed in terms of driving mechanisms for CDW formation: as the conduction band has weight only on 1 out of 13 atoms in the CDW phase, all remaining atoms contribute to the formation of the energetically lowered bands, which could energetically compensate the lattice distortion.

We would like to thank P. Ruffieux, P. Aebi, and M. Göthelid for useful discussions. Skillful technical assistance of E. Mooser, O. Raetzo, R. Schmid, O. Zosso, C. Neururer, and F. Bourqui is gratefully acknowledged. This work has been supported by the Fonds National de la Suisse pour la Recherche Scientifique and Göran Gustafssons Stiftelse.

*stoltz@physics.leidenuniv.nl

[1] H. Ding, T. Yokoya, J. C. Campuzano, T. Takahashi, M. Randeria, M. R. Norman, T. Mochiku, K. Kadowaki, and J. Giapintzakis, Nature (London) **382**, 51 (1996).

[2] A. G. Loeser, Z.-X. Shen, D. S. Dessau, D. S. Marshall, C. H. Park, P. Fournier, and A. Kapitulnik, Science **273**, 325 (1996).

[3] T. Pillo, J. Hayoz, H. Berger, M. Grioni, L. Schlapbach, and P. Aebi, Phys. Rev. Lett. **83**, 3494 (1999).

[4] M. Bovet, D. Popović, F. Clerc, C. Koitzsch, U. Probst, E. Bucher, H. Berger, D. Naumović, and P. Aebi, Phys. Rev. B **69**, 125117 (2004).

[5] C. G. Slough, W. W. McNairy, R. V. Coleman, B. Drake, and P. K. Hansma, Phys. Rev. B **34**, 994 (1986).

[6] J.-J. Kim, W. Yamaguchi, T. Hasegawa, and K. Kitazawa, Phys. Rev. B **50**, 4958 (1994).

[7] B. Giambattista, A. Johnson, R. V. Coleman, B. Drake, and P. K. Hansma, Phys. Rev. B **37**, 2741 (1988).

[8] G. Raina, K. Sater, U. Müller, N. Venkateswaran, and J. Xhie, J. Vac. Sci. Technol. B **9**, 1039 (1990).

[9] W. Han, R. A. Pappas, E. R. Hunt, and R. F. Frindt, Phys. Rev. B **48**, 8466 (1993).

[10] B. Giambattista, C. G. Slough, W. W. McNairy, and R. V. Coleman, Phys. Rev. B **41**, 10082 (1990).

[11] P. Ruffieux, O. Gröning, P. Schwaller, L. Schlapbach, and P. Gröning, Phys. Rev. Lett. **84**, 4910 (2000).

[12] T. Pillo, L. Patthey, E. Boschung, J. Hayoz, P. Aebi, and L. Schlapbach, J. Electron Spectrosc. Relat. Phenom. **97**, 243 (1998).

[13] P. Aebi, J. Osterwalder, P. Schwaller, L. Schlapbach, M. Shimoda, T. Mochiku, and K. Kadowaki, Phys. Rev. Lett. **72**, 2757

(1994).
[14] B. Dardel, M. Grioni, D. Malterre, P. Weibel, Y. Baer, and F. Levý, Phys. Rev. B **45**, 1462 (1992).
[15] J. A. Wilson, F. J. D. Salvo, and S. Mahajan, Adv. Phys. **24**, 117 (1975).
[16] J. Voit, L. Perfetti, F. Zwick, H. Berger, G. Margaritondo, G. Grüner, H. Höchst, and M. Grioni, Science **290**, 501 (2000).
[17] P. Mallet, K. M. Zimmermann, P. Chevalier, J. Marcus, J. Y. Veuillen, and J. M. Gomez Rodriguez, Phys. Rev. B **60**, 2122 (1999).
[18] W. Sacks, D. Roditchev, and J. Klein, Phys. Rev. B **57**, 13118 (1998).
[19] L. Perfetti, A. Georges, S. Florens, S. Biermann, S. Mitrović, H. Berger, Y. Tomm, H. Höchst, and M. Grioni, Phys. Rev. Lett. **90**, 166401 (2003).
[20] S. Colonna, F. Ronci, A. Cricenti, L. Perfetti, H. Berger, and M. Grioni, Phys. Rev. Lett. **94**, 036405 (2005).